Rare Met. (2015) 34(6):440–444
DOI 10.1007/s12598-015-0491-8

RARE METALS
www.editorialmanager.com/rmet

Mineral phase reconstruction behavior of direct reduction and smelting titanium slag at high temperature and slow cooling

**Yi-Jie Wang, Shu-Ming Wen*, Qi-Cheng Feng,
Zhi-Wen Ye, Min Wang**

Received: 19 June 2014 / Revised: 19 October 2014 / Accepted: 2 April 2015 / Published online: 16 May 2015

Abstract Titanium slag in this study was produced by subjecting titanomagnetite concentrate to direct reduction-electric furnace smelting. Processing mineralogy and mineral phase reconstruction behavior at high temperature and slow cooling treatment were examined by chemical analysis, X-ray diffraction (XRD), optical microscopy (OM), scanning electron microscopy (SEM), and energy-dispersive spectroscopy (EDS). Anosovite solid solution is the main titanium product by the direct reduction and smelting process. Results of slow-cooling experiments show that crystal volume and size increase as cooling rate decreases. Anosovite and gangue mineral crystals develop fully with large crystal volume and size at a cooling rate of 2 K·min^{-1}. Moreover, the growth of anosovite crystal was characterized by crystal nucleation and growth theory. These results provide further insights into the separation of anosovite from gangue by mineral processing.

Keywords Direct reduction; Smelting titanium slag; Anosovite; Slow cooling; Crystal

1 Introduction

In China, Panzhihua, Xichang, and Chengde are commonly known for their rich resource of vanadium–titanium magnetite, which contains iron, vanadium, titanium, and other associated metals. However, traditional methods, such as "blast furnace and converter" involving titanomagnetite concentrate, are applicable to the recovery of iron and vanadium, but titanium is not considered in blast furnace slag. Furthermore, the application of blast furnace slag also failed to recover TiO_2. So the TiO_2 in vanadium–titanium magnetite is still lost in blast furnace slag and accounts for 600,000 tons per year [1]. Therefore, researches were prompted to develop new technologies that can be applied to separate and utilize iron, vanadium, and titanium cleanly and efficiently. Third-generation smelting technology, namely "direct reduction and electric furnace smelting," was considerably developed. In this process, titanomagnetite concentrate is directly reduced with coal and then smelted in an electric furnace. Thus, the slag containing TiO_2 approximately 40 %–50 % and direct reduction iron can be achieved. The TiO_2 content of slag is twice as high as that of blast furnace slag. Moreover, the recovery rate of iron increases by 2 %–3 %; by comparison, the recovery rate of vanadium increases by more than 15 % with this technology. As a result, the TiO_2 in direct reduction and smelting titanium slag can be comprehensively utilized [2].

Studies were focused on blast furnace slag [3–9]; however, limited information is available regarding the smelting titanium slag. To develop new process, researchers should consider the recovery of titanium in direct reduction and smelting titanium slag. Yang et al. [10] and Li [11] investigated the acidolysis of smelting titanium slag. Zhang and Zhong et al. [12, 13] performed hydrochloride leaching and "phosphate activation roasting and dilute sulfuric acid

---

Y.-J. Wang, S.-M. Wen*, Q.-C. Feng, Z.-W. Ye
State Key Laboratory of Complex Nonferrous Metal Resources Clean Utilization, Kunming University of Science and Technology, Kunming 650093, China
e-mail: shmwen@126.com

Y.-J. Wang, S.-M. Wen, Q.-C. Feng, Z.-W. Ye
Faculty of Land Resource Engineering, Kunming University of Science and Technology, Kunming 650093, China

M. Wang
Advanced Analysis and Measurement Center, Yunnan University, Kunming 650091, China

leaching" to produce acid-dissolved titanium slag. New utilization methods were also proposed to smelt titanium slag [14–17]. Smelting titanium slag exhibits very complex properties; therefore, several drawbacks result from the direct application of this substance as a raw material in sulfuric acid method to produce titanium dioxide. For example, acidolysis conditions need high requirements, and concentrated acid wastes cannot be used. Impurities, including calcium, magnesium, aluminum, and silicon, are high and very difficult to eliminate; as such, coagulant dosage should be increased and time should be prolonged during acidolysis. Thus, production costs increase and productivity decreases. Nonferrous metals, including vanadium, chromium, and manganese, are also abundantly detected and difficult to eliminate. These elements affect the quality of titanium dioxide [18].

As a consequence, based on "selective enrichment, growth, and separation" theory proposed by Northeastern University [19], "titanium component growth-mineral separation" method was used to the smelting titanium slag. Titanium-bearing phase anosovite and gangue minerals contain fine crystal sizes; as such, these substances are also difficult to separate directly and effectively by beneficiation. Therefore, researchers should develop a reasonable and effective heat treatment process to promote growth and enhance the crystal properties of anosovite and gangue minerals. Mineral crystals should also be transformed from small to large sizes to obtain the necessary conditions for mineral separation. In this research, the processing mineralogy of smelting titanium slag and the effect of cooling rate on mineral phase reconstruction were investigated. This research aimed to recover titanium from smelting titanium slag.

2 Experimental

2.1 Materials

The materials used in the experiment were smelting titanium slag, which were provided by Panzhihua Iron and Steel Group Limited Company in China. They were cooled to room temperature directly from the molten state after electric furnace smelting. The processing mineralogy of smelting titanium slag was examined by chemical analysis, X-ray diffraction (XRD), and optical microscope (OM). Chemical analysis results, XRD patterns, and OM results are shown in Table 1 and Figs. 1 and 2, respectively.

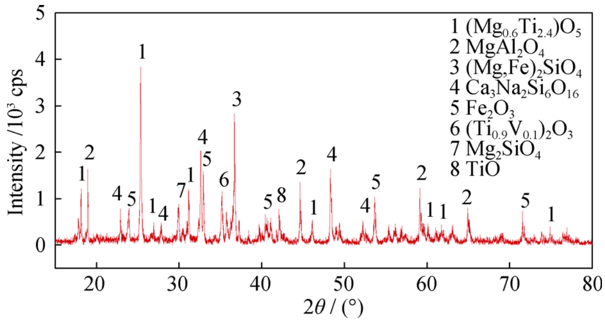

Fig. 1 XRD pattern of materials

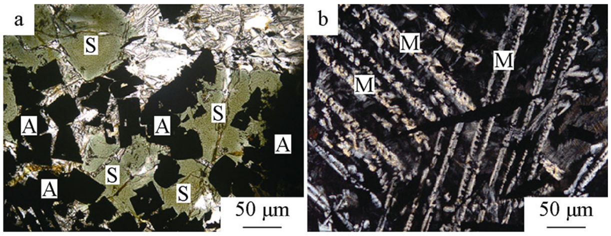

Fig. 2 OM images of materials: **a** spinel (S) and anosovite (A) and **b** melilite (M)

Table 1 shows that the sample contains 46.8 % TiO_2. The contents of iron, manganese, and sulfur are low. By contrast, the contents of harmful elements (vanadium and chromium) and impure elements (aluminum, silicon, calcium, and magnesium) are high. Vanadium and chromium affect the quality of titanium dioxide.

In Fig. 1, anosovite solid solution is the primary useful mineral and can be expressed as follows: $m(AO{\cdot}TiO_2){\cdot}n(B_2O_3{\cdot}TiO_2)$, where A is the divalent titanium, magnesium, iron, manganese, etc., B is the trivalent titanium, iron, aluminum, chromium, etc., m and n are constant coefficient. Moreover, the raw materials contain spinel, hematite, and silicate minerals; among these minerals, anosovite exhibits the highest content, followed by spinel and silicate minerals. XRD patterns show that anosovite crystal is doped with magnesium.

OM images in Fig. 2 show that anosovite, spinel, and melilite coexist in the smelting titanium slag except the glass phase. Anosovite is brown and black and does not exhibit metallic luster. Anosovite mainly appears as an opaque material, but a small portion of this mineral is translucent. Anosovite is observed as columnar, tabular, acicular, and granular. Its content is approximately 50 %, and the particle size ranges from 0.02 to 0.20 mm.

Table 1 Chemical compositions of materials (wt%)

TiO_2	Fe	Mn	Cr	S	V_2O_5	Al_2O_3	SiO_2	CaO	MgO
46.80	1.79	0.54	0.07	0.32	0.82	18.53	17.04	5.66	12.21

2.2 Methods

The experiments were performed in a box-type resistance furnace. The heating element was molybdenum disilicide U-shaped bar. Temperature was controlled by an AI intelligent digital temperature controller with an accuracy of 2 K.

The smelting titanium slag was crushed to 2 mm using a crusher. Approximately 80 g of the sample was transferred into a graphite crucible and placed in a resistance furnace. The temperature of the furnace was increased to 1723 K and then maintained for 30 min. Then the resistance furnace was cooled to 1423 K at the cooling rates of 4.00, 2.00, 1.00, 0.50, and 0.25 $K\cdot min^{-1}$. Then the resistance furnace was closed, and the smelting titanium slag was cooled to room temperature slowly.

After the samples were subjected to heat treatment, the crystal volume and size of the minerals in smelting titanium slag were determined by OM. Mineral crystallization was analyzed using a D/Max2200 XRD analyzer (Rigaku, Japan). Surface micromorphological characteristics were examined using a Quanta 200 scanning electron microscopy (SEM, FEI, the Netherlands). Element contents were determined by Genesis 2000 EDS (EDAX, USA).

3 Results and discussion

3.1 Heating curve

Figure 3 illustrates the curve of temperature versus time during the melting process of the smelting titanium slag. After 280 min of heating, the smelting titanium slag reaches the temperature of 1723 K.

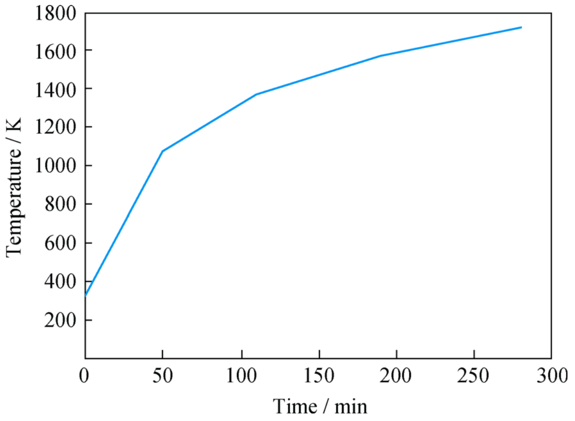

Fig. 3 Heating curve of smelting titanium slag

3.2 OM analysis

After slow-cooling treatment, the samples were prepared as slices and glass slides. Then they were observed by OM to determine the volume and size of anosovite crystal. Semiquantitative analysis results are shown in Table 2. The anosovite crystal volume and size increase as cooling rate decreases. At the cooling rate of $<2\ K\cdot min^{-1}$, crystal volume of 60 % and crystal size of 0.02–1.00 mm are observed, which indicate that slow-cooling treatment is beneficial to the increase in anosovite crystal volume and size.

3.3 XRD analysis

Figure 4 shows the XRD patterns of the smelting titanium slag after the samples were subjected to different cooling rates. Cooling rate significantly affects mineral crystallization. Anosovite and spinel grow and become large in the slow-cooling process. Anosovite and spinel are developed completely, and the main characteristic peaks are evident at a cooling rate of 2 $K\cdot min^{-1}$. Moreover, the chemical formula of anosovite changes from $Mg_{0.6}Ti_{2.4}O_5$ to $MgTi_2O_5$ (Table 3). Mg transfers to anosovite crystal, thereby increasing the stability of crystal lattice and promoting crystal growth.

3.4 SEM–EDS analysis

Figure 5 shows the SEM images and EDS spectra of the raw materials and the smelting titanium slag at 2 $K\cdot min^{-1}$. As can be seen from the SEM images, the minerals are observed mainly as granular with a sharp, and a small number take the form of subhedral tabular and acicular. EDS spectra show that titanium, magnesium, aluminum, silicon, calcium, and other elements in the raw materials are distributed. However, these elements are concentrated at 2 $K\cdot min^{-1}$, which means that the elements in the smelting titanium slag redistribute during the slow-cooling process. Anosovite and spinel crystals grow more completely and contain lower impure elements.

Table 2 Semiquantitative analysis results of OM measurements

Cooling rate/($K\cdot min^{-1}$)	Raw materials	4.00	2.00	1.00	0.50	0.25
Crystal volume/%	∼ 50	± 50	± 55	± 60	± 60	± 60
Crystal size/mm	0.02–0.20	0.02–0.50	0.02–1.00	0.02–1.00	0.02–1.00	0.02–1.00

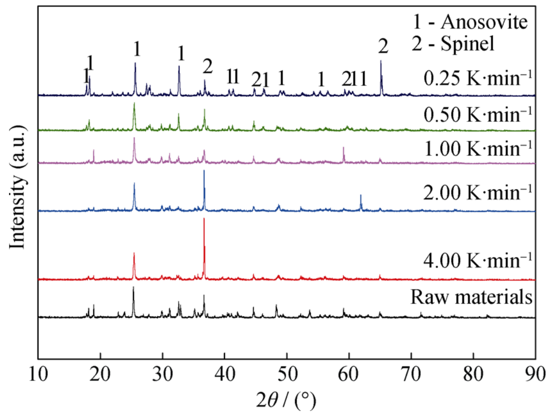

Fig. 4 XRD patterns of smelting titanium slag after different cooling rate treatments

Table 3 XRD results

Cooling rate/($K \cdot min^{-1}$)	2θ/(°)	*hkl*	Phase ID
Raw materials	25.320	110	$Mg_{0.6}Ti_{2.4}O_5$
4.00	25.450	110	$MgTi_2O_5$
2.00	25.460	110	$MgTi_2O_5$
1.00	25.449	110	$MgTi_2O_5$
0.50	25.480	110	$MgTi_2O_5$
0.25	25.591	101	$MgTi_2O_5$

3.5 Mechanism

In thermodynamics, crystallization begins when the melt cools to a temperature less than their corresponding melting points; at such temperatures, the free energy of the solid phase is lower than that of the liquid phase. As a result, the short-range regular structures of liquids form crystal embryos. Crystal embryos with different sizes, which exhibit the same structure as the solid phase, form in the melt. These crystal embryos also attract solute atoms to grow, form crystal nucleus with a certain size, and develop into full crystals. The whole crystallization process involves the formation and growth of crystal nucleus. Cooling rate significantly affects the shape, size, and purity of mineral crystals [20, 21].

3.5.1 Effect of cooling rate on crystal shape

Rapid cooling crystals often develop into columnar, acicular, and scaly structures; such crystals even grow into skeleton-like structures. Under unbalanced conditions, a high energy on crystal surfaces causes an unstable state as a crystal grows, resulting in the growth of skeleton-like crystals along edges or corners. If a crystal grows slowly under almost balanced conditions, a complete crystallized polyhedron usually forms.

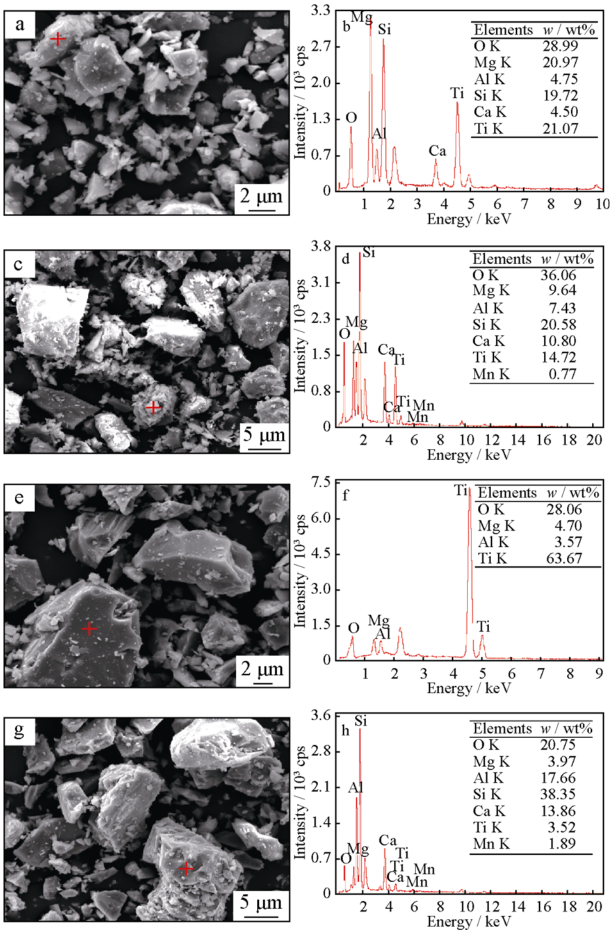

Fig. 5 SEM images and EDS spectra: **a–d** raw materials, **e–h** smelting titanium slag at 2 $K \cdot min^{-1}$

3.5.2 Effect of cooling rate on crystal size

As crystallization occurs in the melt, a fast cooling rate causes the crystal to grow quickly; as a result, numerous crystal nuclei form. However, crystallization completes in a short time and numerous small crystals contain irregular granular aggregations. In addition, solute atoms have insufficient time to adhere to the crystal nucleus and promote crystal growth. Thus, aphanitic minerals and amorphous glass form.

During crystal growth, crystal nuclei absorb one another. Small crystals are also attracted by large ones if the crystal growth rate is slow. Therefore, only a small portion of the crystal nuclei continues to develop. In this case, crystals with ideal structures occupy a large volume.

3.5.3 Effect of cooling rate on crystal purity

Some materials in the melt are included in a crystal when crystals grow rapidly, thereby forming inclusions. Structural defects, which are caused by ion doping in the lattice, deteriorate the purity and integrity of crystals. Ideal crystals can be obtained when crystals grow under almost balanced conditions.

4 Conclusion

The TiO_2 content in the smelting titanium slag is 46.8 %. The common minerals found in the materials include anosovite, spinel, silicate minerals, and glass phase. At a fast cooling rate, the mineral crystal size in the smelting titanium slag is small and exhibits incomplete development.

Cooling rate significantly affects the crystallization of anosovite. Slow cooling is conducive to crystal growth and improves crystal volume and size. After slow cooling treatment is performed, anosovite and gangue minerals in the smelting titanium slag reconstruct and elements redistribute. The size of anosovite and gangue mineral crystals increases and becomes suitable for separation. The most appropriate cooling rate is 2 $K\cdot min^{-1}$.

Acknowledgments This study was financially supported by the Major Program of the National Natural Science Foundation of China (No. 51090385).

References

[1] Li J, Tang XL, Guo M, Zhang M, Zhang ZT, Wang XD. Conditions for extracting anosovite from panzhihua Ti-bearing blast furnace slag. J Chin Rare Earth Soc. 2010;28(S):365.

[2] Yang SL, Sheng JF, Ao JQ. Ilmenite Enrichment. Beijing: Metallurgical Industry Press; 2012. 333.

[3] Li YH, Lou TP, Sui ZT. The effects of heat-treatment on precipitate behavior of the perovskite phase. Acta Metall Sin. 1999;35(11):1130.

[4] Lou TP, Li YH, Li LS, Sui ZT. Study on kinetics of perovskite phase precipitate in slag bearing titanium. J Chin Ceram Soc. 2000;28(3):255.

[5] He CH. Beneficiation experimental research on perovskite in Panzhihua blast furnace slag. Kunming: Kunming University of Science and Technology; 2002. 1.

[6] Fu NX, Zhang L, Cao HY, Sui ZT. Effects of additives on precipitation behavior of perovskite in Ti-bearing blast furnace slag. J Iron Steel Res Int. 2008;20(4):13.

[7] Li YH, Lou TP, Sui ZT. Selective enrichment of Ti component in Ti-bearing blast furnace slag and precipitation behavior of perovskite phase. Trans Nonferrous Met Soc China. 2000;10(5):719.

[8] Wang MY, Zhang L, Zhang LN, Sui ZT, Tu GF. Study on selection of the best titania enrichment phase in titanium-bearing slag. J Mater Metall. 2005;4(3):175.

[9] Li YH, Lou TP, Sui ZT. Effects of CaO and MnO on the crystallization of the perovskite phase in the Ti-bearing blast furnace slag. J Iron Steel Res Int. 2000;12(3):1.

[10] Yang SL, Zhang SL, Ma L, Gao SZ. Experimental study on mineral phase and acidolysis performance of V–Ti–Fe concentrate coal-based direct reduction melting titanium slag. In: Proceedings of Chinese Society for Metals, 2010 Non-blast Furnace Ironmaking Academic Annual Meeting and Comprehensive Utilization Seminar of Titanomagnetite, Panzhihua; 2010. 347.

[11] Li L. Research on the acidolysis technology of Panzhihuan vanadic titanomagnetite deeply reducing slag. Light Metals. 2010;5:50.

[12] Zhang SL, Bai GH, Liu QS, Luo Y, Yuan B, Wang YJ, Wang HB, Sun QZ. A preparation method of acid dissolved titanium slag with direct reduction melting titanium slag by hydrochloric acid leaching. China Patent; CN 102887542 A. 2013.

[13] Zhong BN, Xue TY, Hu GP, Chen WL, Wang LN, Qi T. Enrichment of low grade reduced titanium slag by H_3PO_4 activation roasting and acid leaching. The Chinese Journal of Process Engineering. 2013;13(3):378.

[14] Liu SL, Zhang XF, Fang MX, Fu C, Li G, Chen WM. A preparation method of rich titanium product with V-Ti-Fe concentrate direct reduction melting titanium slag. China Patent; CN 102787194 A. 2012.

[15] Cai PX, Zhang SG, Deng BS, Lin FR, Dai TJ, Chang J. A preparation method of rutile titanium dioxide with melting titanium slag. China Patent; CN 101898791 A. 2010.

[16] Cai PX, Zhang SG, Deng BS, Lin FR, Dai TJ, Yuan SL. A preparation method of titanium dioxide with melting titanium slag and titanium concentrate by acidolysis. China Patent; CN 101857269 A. 2010.

[17] Mei WD. A preparation method of ferrotitanium with melting titanium slag. China Patent; CN 1827787A. 2006.

[18] Yang SL, Sheng JF, Ao JQ. Ilmenite Enrichment. Beijing: Metallurgical Industry Press; 2012. 335.

[19] Sui ZT, Guo ZZ, Zhang L, Zhang LN, Wang MY, Lou TP, Li GQ. Green separation technique of Ti component from Ti-bearing blast furnace slag. J Mater Metall. 2006;5(2):93.

[20] Yao LZ. Crystal growth foundation. Hefei: University of Science and Technology of China Press; 1995. 412.

[21] Liu YY, Liu FS. Phase transformation behavior of $Ti_{49}Ni_{49.5}$-$Fe_1V_{0.5}$ and $Ti_{48}Ni_{48.5}Fe_1V_{2.5}$ alloys after different heat treatments. Rare Met. 2014;33(1):16.